A Surface Temperature Estimation Method for Lithium-ion Battery Using Enhanced GRU-RNN

Qi Yao, Dylan Dah-Chuan Lu, *Senior Member, IEEE,* Gang Lei, *Senior Member, IEEE,*

***Abstract*—To monitor the thermal performance of the battery, the surface temperature (ST) of the battery is normally directly measured by temperature sensors. As the number of battery cells or strings increases, the number of temperature sensors increases proportionally. This increases the cost and reduces the reliability of the battery systems. To solve this problem, this paper introduces a method to accurately estimate the ST of lithium-ion batteries using a recurrent neural network (RNN) with gated recurrent unit (GRU). Firstly, this paper analyzes the battery ST distribution theory and proves that it is a time-series task since the present ST is conditioned on the previous state. Secondly, a GRU-RNN model is adopted to estimate battery ST as this model has the ability to automatically encode dependencies in time and accurately estimate battery ST without using any physical battery models or filters. Thirdly, an improved data normalization method is proposed to enhance the estimation accuracy and robustness. Fourthly, the proposed data normalization method is incorporated into the stacked GRU-RNN to estimate the battery ST from compulsory online signals. The proposed method is verified with $LiFePO_4$ using US06 and FUDS profiles under four fixed ambient temperatures and with $LiNiCoAlO_2$ using a mixed dynamic profiles under a varying ambient temperature range (from 10°C to 25°C). The estimation error using MAE is less than 0.2°C over the all fixed ambient temperature conditions, and 0.42°C over the varying ambient temperature condition.**

***Index Terms*—Battery temperature estimation, lithium-ion battery, recurent neural network, gated recurrent unit**

I. Introduction

TEMPERATURE monitoring is one of the most important functions of the battery management system to ensure particularly electro-thermal stability of batteries [1], [2]. In general, the temperature measurement is used for three conditions: stationary storage, charging, and discharging. To achieve thermal monitoring, avoid over-heat issues, and update temperature-dependent parameters, the battery temperature needs to be monitored and controlled within an allowable temperature range. Moreover, the lithium-ion battery is sensitive to temperature variations, so it is necessary to update battery parameters with the temperature change [3], [4]. For example, the available battery capacity becomes smaller with decreasing ambient temperature.

Typically, the battery surface temperature (ST) can be directly measured by temperature sensors. Commonly used temperature sensors for battery temperature measurement have the thermal properties of Negative Temperature Coefficient (NTC) (metal oxide) or Positive Temperature Coefficient (PTC) (semiconductor type) [5]. The resistance of these types of sensors changes as a function of the temperature, and its voltage drop across the sensor is an indicator of the temperature. This type of sensors is relatively cheap, but they exhibit nonlinear characteristic in high and low-temperature regions. Moreover, digital interfaced sensors, which facilitates the integration and communication with microprocessors and controllers, are also common for temperature measurement. However, the sensors installation, cabling, and signal acquisition will increase the cost and decrease the system reliability as these additional components are also prone to failure [2].

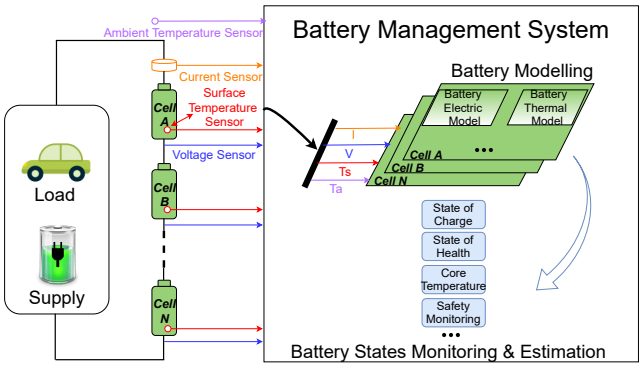

(a)

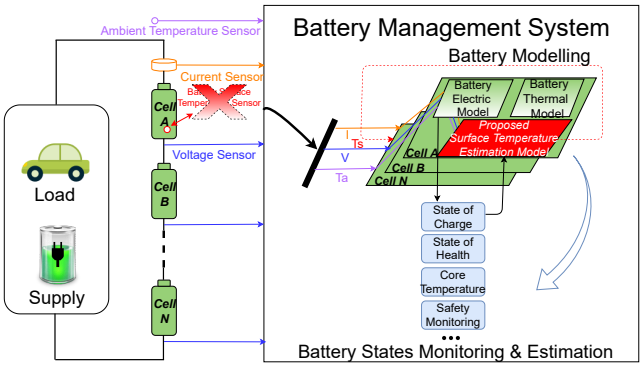

(b)

Fig. 1. Illustration diagram of the battery management system: signal acquisition, battery modelling, and states estimation. (a) The conventional signal acquisition system requires *N* voltage sensors, *1* current sensor, *N* surface temperature sensor, and *1* ambient temperature sensor. (b) The work adopting the proposed requires: *N* voltage sensors, *1* current sensor, and *1* ambient temperature sensor.

To overcome problems brought by sensors, some sensorless battery temperature estimation methods have been proposed [1], [2], [6], [7]. For example, an equivalent circuit-based method has been proposed in [6]. In this method, a reduced-order battery thermal circuit and a Kalman filter were adopted

Q. Yao, D. D.-C. Lu and G.Lei are with the Faculty of Engineering and Information Technology, University of Technology Sydney, Sydney, NSW 2007, Australia.

to estimate the temperature. This method, however, requires the comprehensive pre-knowledge of the cell thermal characteristics, thermal boundary conditions, and heat generation rates. Other typical methods, which use the electrochemical impedance spectroscopy of the battery to estimate the battery surface temperature, have been proposed [2], [7]. These methods utilized the relationship between the temperature and battery impedance, which can be obtained by injecting a small ac current to the battery and observing its corresponding voltage response. However, these methods usually require extra hardware design to measure battery impedance [8], [9].

As computing power and available data increases, the machine learning (ML)-based methods have since applied in battery systems. For example, ML-based strategies have been widely discussed in battery state of charge (SOC) estimation field [10]. A b ack p ropagation (BP) n eural n etwork [11], in which the measured battery current, terminal voltage, and ambient temperature are used as the input and the SOC as the output for SOC estimation task. As the SOC estimation is a typical time sequence task, recurrent neural network (RNN) has a special internal structure to process sequence tasks. Therefore, RNNs have been widely adopted for SOC estimation [12], [13]. Moreover, ML-based techniques have also been widely applied to estimate the state of health (SOH) and remaining useful lifetime (RUL) of the battery [14]. For example, Gaussian Process Regression and Support Vector Machine model-based approaches are proposed to estimate SOC and SOH [14].

Similar to the SOC estimation task, the ML-based method has offered an alternative solution for battery surface temperature estimation, as this method treats the battery as a black box and directly learns its internal dynamics through large amounts of datasets to establish the nonlinear relationship between the input signals and output signals. A sensorless ST estimation method using the traditional artificial n eural n etwork (ANN) has been proposed [1]. Nevertheless, there are three problems associated with this method. First, it is known that temperature a slow varying parameter. Therefore, the battery surface temperature under the present time-step is conditioned based on its previous state. But the structure of the ANN lacks the ability to memorize previous information. Therefore, it needs the system to re-send previous battery operational data to present step for computation. It definitely i ncrease t he o perational complexity and reduce the computational efficiency. T o o vercome this issue, a recurrent neural network (RNN) have been proposed to estimate the battery surface temperature [15]. However, this method lacks theoretical analysis about the connection between battery temperature distribution and neural network models.

To promote the application of sensorless techniques and overcome aforementioned issues in previous work [1], [6], the RNN should be adopted for battery ST estimation as RNN has the ability to make use of important historical information for the present state estimation. Nonetheless, the original RNN or so called simple RNN (SRNN) is incapable of capturing long-term dependencies due to the gradient vanishing or rare gradient explosion phenomenons during the back-propagation process [16]. More advanced structures have been proposed to address this disadvantage of the SRNN, such as LSTM, GRU and BiRNN [12], [16]. Among these advanced RNN structures, the GRU unit, which was proposed by Kyunghyun et al. in 2014 [17], shows its advantages that the GRU unit not only can handle the long-term sequential dependencies but also has a simpler internal structure [17].

This paper therefore proposes a sensorless battery ST estimation method using an GRU-RNN, as shown in Fig. 1. A GRU-RNN is designed to estimate the battery ST, which is based on the fact that the battery thermal model is a complex and nonlinear system and the procedure of battery surface temperature estimation is a time series task. As an enhanced structure of RNN, the GRU-RNN not only can inherit the advantages of traditional RNN, but also can selectively memorize the useful information and discard the redundant information. Therefore, it can achieve a high estimation accuracy with a low computational complexity. The main contributions and salient features of this work are summarised as follows:

1) This paper firstly analyses the theoretical relationship between the battery ST and RNN by proving that the battery temperature distribution is a time series task.
2) A GRU-RNN, whose structure is simple and has advantages in time series task processing, is first introduced to estimate battery ST. And an improved input data normalization method is proposed to cooperate with the GRU-RNN network to enhance ST estimation accuracy and robustness.
3) The proposed GRU-RNN network was trained and validated under dynamic driving profiles with various fixed ambient temperature. To mostly mimic the real operational conditions of electric vehicles (EVs), it is evaluated by a combined driving profiles under a varying temperature condition (from 10°C to 25°C). And the experimental results revealed that the proposed network can achieve a high accuracy in all conditions. Moreover, a series of uncertainty analysis, which considered signal sampled errors have been applied to the network, the results shows that estimation error is 10% larger than ideal condition.

After a brief introduction, Section II introduces the time-series characteristics of battery temperature distribution. Section III introduces the architecture of RNN , GRU cells, and the GRU-RNN network with the proposed normalization techniques. Section IV gives the specification of cells, the experimental platform used for data acquisition, and the experimental data pre-processing method. In Section V, the performance of the proposed a GRU-RNN network is validated on different fixed temperature conditions and a varing temperature conditions. Finally, the conclusion is given in Section VI.

II. Battery Temperature Time-Series Characteristic Analysis

A commonly adopted expression for the heat generation (Q) in a lithium-ion battery is

$$Q = I\left(V_B - OCV\right) \tag{1}$$

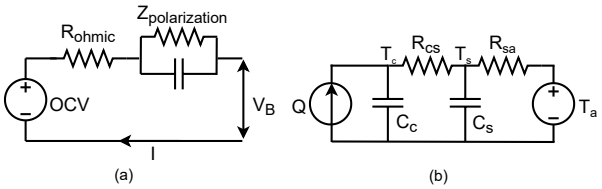

Fig. 2. (a) Battery equivalent circuit electric model. (b) Battery equivalent circuit thermal model.

which is a simplified equation proposed by Bernardi *et al.* [18]. The term at the right side is the heat generated by the ohmic resistance and charge transfer overpotential [6], which have been represented as R_{ohmic} and $Z_{polarization}$ in Fig. 2(a). Furthermore, I and V_B are the current and terminal voltage of the battery respectively, which can be directly measured online by physical sensors. OCV, which is the open-circuit voltage of the battery under an inner-equilibrium-state, has a direct relationship with the battery SOC.

To simplify the thermal analysis, two assumptions should be made: (a) the generated heat is uniformly distributed; (b) the battery surface temperature is uniform. Fig. 2(b) shows a simplified battery equivalent circuit thermal model, which can be used to express the relationship between heat generation and battery temperature.

$$\begin{aligned} C_c\frac{dT_c}{dt} &= Q - \frac{T_c - T_s}{R_{\text{cs}}} \\ C_s\frac{dT_s}{dt} &= \frac{T_c - T_s}{R_{\text{cs}}} - \frac{T_s - T_a}{R_{\text{sa}}} \end{aligned} \tag{2}$$

where C_c and C_s are the battery heat capacity of the core and surface respectively, T_c and T_s are the battery temperature of the core and surface, T_a is the ambient temperature, R_{cs} is the core-to-surface resistance of the battery, and R_{sa} is the surface-to-ambient resistance of the battery.

To better explain why the ST distribution is a time series task, (1) and (2) are expressed as a state function of a continuous time dynamic system.

$$\begin{bmatrix} \dot{T}_c \\ \dot{T}_s \end{bmatrix} = \begin{bmatrix} -\frac{1}{C_c R_{cs}} & \frac{1}{C_c R_{cs}} \\ \frac{1}{C_c R_{cs}} & -\frac{2}{C_c R_{cs}} \end{bmatrix} \begin{bmatrix} T_c \\ T_s \end{bmatrix} + \begin{bmatrix} 0 & \frac{1}{C_c} \\ \frac{1}{C_s R_{sa}} & 0 \end{bmatrix} \begin{bmatrix} T_a \\ I(V_B - OCV) \end{bmatrix} \tag{3}$$

Based on above states equations, it can be observed that the battery surface temperature of the next time-step ($\dot{T}_s$) is conditioned on its inherent chemical characteristics of the battery (C_c, C_s, R_{cs}, and R_{sa}), heat generation and ambient temperature (Q, and $T_{a,k}$), and the present surface temperature (T_s). And the heat generation is calculated by the operational current (I), battery terminal voltage (V_B), and open circuit voltage (OCV). As SOC has a one-to-one correspondence with OCV [19], and this correspondence can be expressed as a nonlinear function. Thus, SOC can be used to represent OCV for heat analysis. From the above analysis, it is clearly that the battery ST is a typical time series task.

However, this simplified thermal model is used to describe the time series characterises of the ST distribution. To achieve a high temperature estimation, it is necessary to adopt numerical electrical-thermal models or a one-dimensional cylindrical heat equation with a polynomial approximation [6].

III. Recurrent Neural Network Architecture

RNNs, which are a type of supervised machine learning models, are made of neurons with feedback loops [20]. The feedback loops perform recurrent cycles over time or sequence, as shown in Fig. 3. The structure of RNNs enables it to store and remember past signals for long time periods. Moreover, RNNs can map an input to the output at the present time-step and make prediction in the next time-step. Recently, RNNs have been widely adopted in speech recognition, translation, and stock forecasting fields with promising results and performance [21].

A. Architecture of A Simple Recurrent Neural Network

The hidden layer defines the historical information or memory, which is called hidden state (h), and update function is given as:

$$\mathbf{h}_t = \mathbf{g}_1\left(\mathbf{W}_{hh}\mathbf{h}_{t-1} + \mathbf{W}_{hx}\mathbf{x}_t + \mathbf{b}_h\right) \tag{4}$$

$$\mathbf{y}_t = \mathbf{g}_2\left(\mathbf{W}_{yh}\mathbf{h}_t + \mathbf{b}_y\right) \tag{5}$$

where $\mathbf{W}_{hh}$, $\mathbf{W}_{hx}$, $\mathbf{W}_{yh}$ are distinct weight matrix between layers, $\mathbf{b}_h$ and $\mathbf{b}_y$ are the bias parameter of the node, $\mathbf{g}_1$ and $\mathbf{g}_2$ are activation functions, and $\mathbf{y}_t$ is the output of the RNN network.

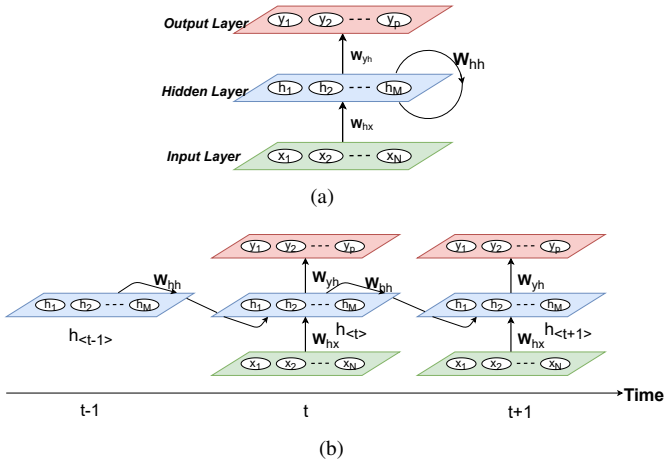

Fig. 3. Illustration diagram of SRNN principle: x is the input vector, h is the hidden state, and y is the output vector

As point out by Benigo [22], the SRNN lacks the ability to capture long-term dependencies during the back-propagation process when the input sequence gets longer. An advanced architecture, so called GRU unit, which not only inherits the advantages in processing time-series task but also overcomes its disadvantages for vanishing gradient phenomenon during the back-propagation process is proposed.

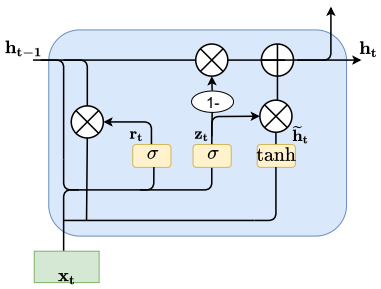

Fig. 4. GRU cell structure.

B. Architecture of A Recurrent Neural Network with Gated Recurrent Unit

The architecture of a GRU cell is given in Fig. 4. For GRU-RNN, the present $\mathbf{h}_t$ is not directly calculated by the previous hidden state $\mathbf{h}_{t-1}$ and the present input $\mathbf{x}_t$ by a constant equation. Instead, the GRU cell is formed by two gates, which are reset gate and update gate, respectively. The update gate ($\mathbf{z}_t$) is used to decide how much of past information should be passed along to the future state. The reset gate ($\mathbf{r}_t$) is used to decide how much of the past information should be discarded. For a time-series dataset, the calculation procedures of GRU are

$$\mathbf{z}_t = \sigma\left(\mathbf{W}_{xz}\mathbf{x}_t + \mathbf{U}_{hz}\mathbf{h}_{t-1} + \mathbf{b}_z\right) \tag{6}$$

$$\mathbf{r}_t = \sigma\left(\mathbf{W}_{xr}\mathbf{x}_t + \mathbf{U}_{hr}\mathbf{h}_{t-1} + \mathbf{b}_r\right) \tag{7}$$

$$\tilde{\boldsymbol{h}_t} = \tanh\left(\boldsymbol{W}_{xc}\boldsymbol{x}_t + \boldsymbol{U}_{hc}\left(\boldsymbol{r}_t \odot \boldsymbol{h}_{t-1}\right) + \boldsymbol{b}_c\right) \tag{8}$$

$$\boldsymbol{h}_t = \left(1 - \boldsymbol{z}_t\right) \odot \boldsymbol{h}_{t-1} + \boldsymbol{z}_t \odot \tilde{\boldsymbol{h}_t} \tag{9}$$

where $\mathbf{W}_{xz}$, $\mathbf{W}_{xr}$, and $\mathbf{W}_{xc}$ are the weights between the input layer and the update gate, reset gate, and candidate layer, respectively; $\mathbf{U}_{hz}$, $\mathbf{U}_{hr}$, and $\mathbf{U}_{hc}$ are the weights between the present time-step t and the previous time-step t$-$1; and $\mathbf{b}_z$, $\mathbf{b}_r$, and $\mathbf{b}_c$ are the biases of the update gate, reset gate, and the candidate state in the GRU unit, respectively. Fig. 4 and above equations show that σ function is used to compute the gate activation, and $tanh$ function is sued to compute the state activation function. And they are defined as:

$$\sigma(\mathbf{x}) = \frac{1}{1 + e^{-x}} \tag{10}$$

$$\tanh(\mathbf{x}) = \frac{e^{x} - e^{-x}}{e^{x} + e^{-x}} \tag{11}$$

C. A Stacked GRU-RNN with Proposed Novel Normalization Techniques

As aforementioned, the RNN model has advantages in solving time series task as its structure can understand sequential dependencies. In particular, RNN with GRU unit can selectively remember important information over time to achieve a high accuracy and reduce the computational complexity. Therefore, this paper presents a GRU-RNN model for battery ST estimation. From (1)-(3), it is known that the battery ST has a complicated relationship with battery current, battery SOC, and ambient temperature. And all these signals are compulsory signals for the battery management system, so it can be directly used for ST estimation to reduce the cost and improve the reliability of the battery sensing system.

In a GRU-RNN model, the first layer should be a sequence input layer, in which the measured signals including battery voltage, battery current, battery SOC, and ambient temperature are formed into an input vector $\mathbf{x}_t$ = [$V_B(t)$, $I(t)$, $SOC(t)$, $T_a(t)$]. However, these input varaibles have largely different numeric interval. For example, under a dynamic discharging condition, the range of battery voltage is between 2.0 to 3.6 V ($LiFePO_4$) or 2.5 to 4.2 V ($LiNiMnCoO_2$). And the value of battery current can be up to 6.8 A for a single Panasonic NCR18650 cell. Differences in the scales across these input variables may increase the difficulty of the ST being modeled. To achieve a stable and fast learning process, the input columns should be normalized within proper intervals before forming into a input vector. In previous work, all input columns are normalized by the same min-max normalization method to estimate the output, such as SOC estimation [23]–[25]. However, by analysing the correlation of inputs and output, this paper presents a hybrid normalization method, in which the battery current is normalized between [-1, 1] by adopting (12), the battery voltage and ambient temperature is normalized between [0, 1] by adopting (13), and the battery SOC does not need to be normalized due to its real value is from 0 to 1.

$$x' = \frac{2 \times (x - x_{min})}{x_{max} - x_{min}} - 1 \tag{12}$$

$$x' = \frac{x - x_{min}}{x_{max} - x_{min}} \tag{13}$$

where x_{min} and x_{max} are the minimum and maximum values of datasets, x is the present value.

The width of the input sequence layer is the same as the dimension of the input vector ($\mathbf{x}_t$). Then, a following GRU layer is used to learn the dependence on the information of the previous ST (stored in $\mathbf{h}_{t-1}$) and the present input vector ($\mathbf{x}_t$), as described in (6)-(9). Moreover, more GRU layers can be stacked into a deep neural network for a better learning process. Finally, a fully connected layer is adopted to achieve a linear transformation on the hidden states to the output. This process is done by the following equation:

$$\hat{\mathbf{T}}_{s,k} = \sigma\left(\mathbf{U}_{yh}\mathbf{h}_t + \mathbf{b}_y\right) \tag{14}$$

where $\mathbf{U}_{yh}$ and $\mathbf{b}_y$ are weight matrix and biases of the fully connected layer. The error between the GRU-RNN estimated ST and the sensor measured is represented by the following loss function, which is computed at the end of each forward pass:

$$\mathbf{L} = \sum_{t=0}^{N} \frac{1}{2}\left(\mathbf{T}_{s,t} - \hat{\mathbf{T}}_{s,t}\right)^2 \tag{15}$$

where N is the length of the sequence, $\mathbf{T}_{s,t}$, and $\hat{\mathbf{T}}_{s,t}$ are the ground truth and estimated values of battery ST at time step t.

IV. Description of Datasets

In this study, two publicly available datasets are utilized to evaluate the proposed GRU-RNN model. It should be mentioned that there is a review paper summarised and listed all well-known lithium-ion batteries testing datasets [26].The experimental samples are two types of cylindrical 18650 lithium-ion cells, and their detailed specifications are given in Table I. In particular, the battery materials in the two datasets are different, so it can better verify the general adaptation of the GRU-RNN model. The experimental platform consists of a battery tester, a climate chamber and a PC with a testing software. To measure the surface temperature of the battery cell, a temperature sensor is mounted near the center of the cell surface using thermal paste and tape [23].

TABLE I
SPECIFICATIONS OF THE BATTERIES IN THE EXPERIMENT

Source	Type	Material	Voltage/ V	Capacity / Ah
Dataset1	A12318650	$LiFePO_4$	2.0-3.6	1.1
Dataset2	Panasonic18650	$LiNiCoAlO_2$	2.5-4.2	2.9

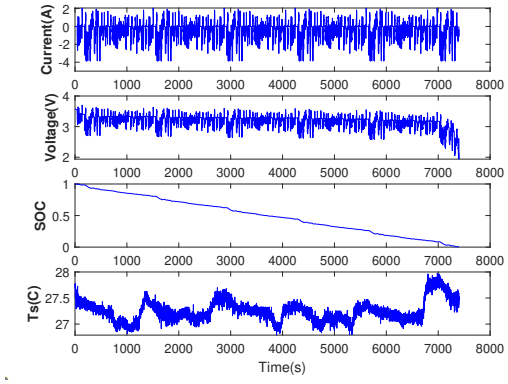

(a)

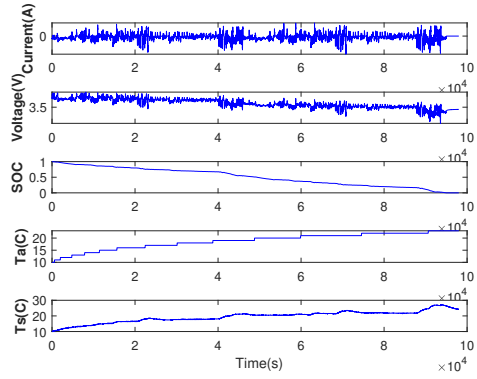

(b)

Fig. 5. Illustration of two datasets: (a) FUDS drive cycle under 25°C in dataset1: Current, Voltage, SOC and Surface Temperature (b) dataset2: Current, Voltage, SOC, Ambient Temperature, and Surface Temperature

The first dataset was collected from the Center for Advanced Life Cycle Engineering (CALCE) of the University of Maryland [23]. The practical driving scenarios of EVs are uncertain and complicated. To mostly mimic real operational conditions, two practical driving profiles are applied on batteries for testing: the Federal Urban Driving Schedule (FUDS) and the US06 Highway Driving Schedule [23]. In these tests, the battery cell is fully charged to 100% SOC at 3.6 V. And the specific dynamic profile is applied to the battery cell until reaching the batteries' cut-off voltage (2.0 V) over several cycles. Since the performance of the battery is highly influenced by the environmental temperature [23], it is necessary to repeat the experiment under a wide range ambient temperature conditions ($-10°$C, $0°$C, $25°$C, and $50°$C). To provide an example, Fig. 5 plots the profiles of battery current, battery terminal voltage, SOC, and battery surface temperature with FUDS under $25°$C.

The second dataset was collected from the Univeristy of Wsiconsin-Madison [12]. Since the dynamic estimation ability under different fixed temperature has been verified by adopting the first dataset. However, the performance of the proposed GRU-RNN at a varing temperature condition remains problem. Hence, in the second dataset, the battery cell is exposed to a varing ambinet temperature from $10°$C to $25°$C. Similar to the first dataset, the battery is fully charged by CCCV method, then discharged by a combination of several driving profiles, which are Urban Dynamometer Driving Schedule (UDDS), Los Angeles 92 (LA92), Supplemental Federal Test Procedure Driving Schedule (US06), and Highway Fuel Economy Driving Schedule (HWFET). Fig. 5(b) plots the profiles of battery current, battery terminal voltage, SOC, ambient temperature, and battery surface temperature.

To train the GRU-RNN model, a typical data preparation method in machine learning field is adopted in this paper. Specifically, 70% of experimental data are chosen to train the neural network, and the 15% experimental data are used to validate the accuracy of the trained network during the training process. The aim of validation is to generate a feedback to update model parameters. Once the model is successfully trained, the reminding 15% data are used to test its estimation accuracy. As aforementioned, the datasets should be normalized using the proposed method before sending for the training process.

V. Proposed GRU-RNN Model Evaluation

As aforementioned, the input vector fed into the improved GRU-RNN is defined as $\mathbf{x}_t = [V_B(t), I(t), SOC(t), T_a(t)]$. The output of the improved GRU-RNN model is the surface temperature at time step t, which is expressed as $\hat{\mathbf{T}}_{s,t}$. The true value of surface temperature is measured by a sensor, and it is expressed as $\mathbf{T}_{s,t}$ at time step t. The proposed model accuracy can be evaluated by three criterion: root mean square error (RMSE), mean absolute error (MAE). and max error (MAXE), which are expressed as follows:

$$\mathrm{RMSE} = \sqrt{\frac{1}{N}\sum_{t=1}^{N}\left(T_{s,t} - \widehat{T}_{s,t}\right)^2} \tag{16}$$

$$\mathrm{MAE} = \frac{1}{N}\sum_{t=1}^{N}\left|T_{s,t} - \widehat{T}_{s,t}\right| \tag{17}$$

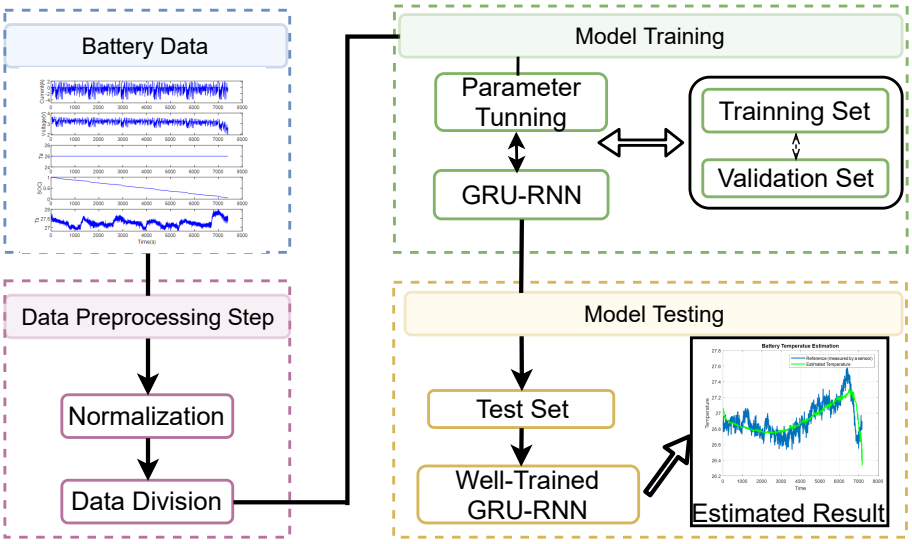

Fig. 6. Experimental procedure for GRU-RNN model training and temperature estimation.

TABLE II
TEMPERATURE ESTIMATION RESULTS WITH THE PROPOSED GRU-RNN

		Layer=1						Layer=2		Layer=3	
Hidden Neurons	Number	4	8	16	32	64	128	8	16	8	16
RMSE	in °C	0.0963	0.0930	0.0932	0.0938	0.0935	0.0940	0.0880	0.0879	0.0877	0.0881
	Normalized Form	6.97%	6.72%	6.74%	6.78%	6.76%	6.79%	6.36%	6.33%	6.31%	6.37%
MAE	in °C	0.0765	0.0732	0.0738	0.0746	0.0742	0.0748	0.0694	0.0697	0.0689	0.0693
	Normalized Form	5.53%	5.30%	5.34%	5.40%	5.37%	5.41%	5.01%	5.04%	4.93%	5.01%
MAXE	in °C	0.395	0.401	0.392	0.391	0.397	0.388	0.3101	0.3035	0.3057	0.3113
	Normalized Form	28.6%	28.9%	28.5%	28.3%	28.4%	28.0%	22.4%	21.9%	22.1%	22.5%
Model Size	KB	1.90	2.64	4.76	11.8	38.8	142	4.32	10.6	6.26	16.5

$$\text{MAXE} = Max\left|T_{s,t} - \widehat{T}_{s,t}\right| \tag{18}$$

where N is the length of the dataset. The RMSE indicates the robustness of the estimation, MEA and MAXE specify the accuracy of the estimation.

Since the possible accuracy of the GRU-RNN is decided by the setting of model parameters, so it is important to explore different network settings to achieve the highest estimation accuracy. For a GRU-RNN model, the basic parameters are the number of layers and the number of hidden nodes per layer. Some advanced settings are the mini-batch size, the drop-out rate among layers, and the learning rate of the model training, etc.

Some of the parameters during the training process are initialized as follows:

* training epoch: 1000
* mini-batch size: 256
* learning rate dropout rare: 20% per 200 epoch
* gradient threshold: 1
* optimizer: Adam
* dropout layer: 0

All the training processes are run on a computer with a single RTX 3090 GPU. The whole experimental flow-chat is given in Fig.6.

A. ST Estimation at Different Fixed Ambient Temperature Conditions

To establish the proposed GRU-RNN model, the size of the input sequence layer and output layer are the same as the dimension of the input vector and output data, which should be four and one, respectively. However, when the battery is operated under a fixed ambient temperature condition, namely, T_a is a constant value, which can be neglected for model training. Hence, the the dimension of the input sequence layer is only three for this case. The number of hidden neurons decides the 'width' of the model, the number of layers decides the 'depth' of the model. So their numbers should be carefully tuned by grid searching.

A GRU-RNN model, which has different hidden GRU layers with different hidden neurons for each layer, is trained and tested with the initialized parameters using FUDS profiles under $-10°$C, which belongs to dataset1. Multiple consecutive powers of 2 are adopted to set the number of hidden neurons, and it is a commonly adopted neuron setting method [27]. The experimental results are given by Table II. When the GRU-RNN network has one layer, the RMSE is improved from 0.0963°C with 4 nodes to 0.0930°C with 8 nodes. Subsequently, the estimated accuracy gradually declines to 0.0940°C with 128 nodes. When the GRU-RNN model has

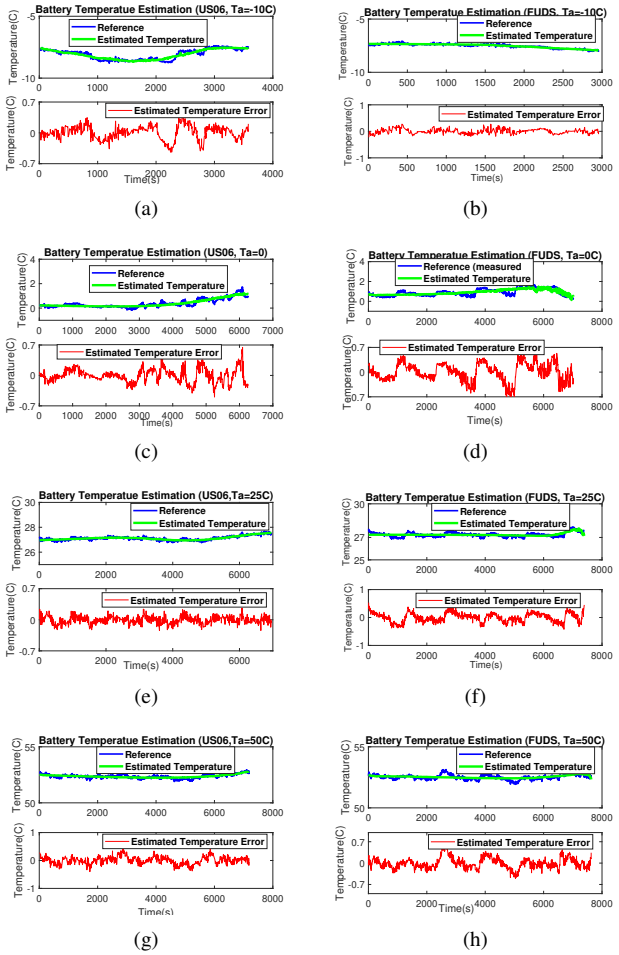

Fig. 7. Temperature estimation with GRU-RNN network with the proposed normalization method under different different loading profiles and temperature from: (a) US06 at $-10°$C; (b) FUSA at $-10°$C; (c) US06 at $0°$C; (d) FUDS at $0°$C; (e) US06 at $25°$C; (f) FUDS at $25°$C; (g) US06 at $50°$C; (h) FUDS at $50°$C;

only one hidden layer, the highest accuracy is achieved by the layers with 8 and 16 hidden neurons. Then, more layers with 8 and 16 nodes are constructed to a stacked GRU-RNN model. The final results show that the GRU-RNN model has 3 hidden layers with 8 hidden neurons ("8-8-8") has the best estimation performance, which is evaluated by RMSE, MAE, and MAXE, respectively. Moreover, the model size of the well trained GRU-RNN is only 6.26 KB, which is easily to be embedded to the chip for online computation.

The aforementioned experiments indicate that the stacked GRU-RNN with few hidden layers and few hidden neurons can perform accurate ST estimation. The reason is that the dimension of the input vector is small, so few hidden neurons are enough to capture the nonlinear characterises inside the battery. Otherwise, the model tends to be over-fitting with too many hidden layer or hidden neurons. Moreover, it is known that Long-short term memory (LSTM)-RNN is also widely used to process the time-series tasks. It is also necessary to compare the performance of the proposed GRU-RNN and LSTM-RNN in processing battery ST estimation. And the experimental results are given in Table III. Therefore, the

TABLE III
COMPARISON OF LSTM-RNN AND GRU-RNN WITH FUDS UNDER -10°C CONDITION

Item	LSTM-RNN1	LSTM-RNN2	GRU-RNN1	GRU-RNN2
MEA°C	0.0714	0.0691	0.0740	0.0689
RMSE°C	0.0926	0.0891	0.0883	0.0877
MAXE°C	0.3141	0.2703	0.2725	0.3057
Size	7.71KB	7.70KB	6.25KB	6.26KB
Training Time	4mins58s	5mins7s	5mins3s	5mins3s
Testing Time	0.092s	0.0689s	0.0543s	0.0433s

LSTM-RNN1 and GRU-RNN1 are the "8-8-8" models with the normal normalization method
LSTM-RNN2 and GRU-RNN2 are the "8-8-8" models with the hybrid normalization method

TABLE IV
ST ESTIMATION RESULTS WITH THE GRU-RNN USING THE PROPOSED NORMALIZATION TECHNIQUES AND CONVENTIONAL TECHNIQUES

	Profiles	US06		FUDS	
	Model	**Method 1**	Method 2	**Method 1**	Method 2
-10°C	MAE($°C$)	0.1218	0.1251	0.0689	0.0740
	RMSE($°C$)	0.1550	0.1581	0.0877	0.0883
	MAXE($°C$)	0.4398	0.4480	0.3057	0.2725
0°C	MAE($°C$)	0.1220	0.1237	0.2039	0.2127
	RMSE($°C$)	0.1580	0.1589	0.2506	0.2607
	MAXE($°C$)	0.5993	0.6452	0.7385	0.8737
25°C	MAE($°C$)	0.0661	0.0681	0.1397	0.1442
	RMSE($°C$)	0.0835	0.0859	0.1737	0.1759
	MAXE($°C$)	0.2605	0.3423	0.4635	0.4950
50°C	MAE($°C$)	0.1057	0.1103	0.1411	0.1414
	RMSE($°C$)	0.1339	0.1348	0.1828	0.1829
	MAXE($°C$)	0.4469	0.4479	0.6422	0.6514

Method 2 (reference normalization method) is present in [23], [25]

"8-8-8" GRU-RNN structure with the proposed normalization method is adopted for the following experiment.

Since ambient temperature has a significant influence on ST estimation, the proposed GRU-RNN network should be verified under different fixed ambient temperature conditions. Fig.7 and Table III show the measured, estimated temperature and the estimation error with US06 and FUDS loading profiles under $-10°$C, $0°$C, $25°$C and $50°$C ambient temperature conditions, respectively. The results in Fig.7 and Table IV show that the proposed network has a better performance in US06 operational profile. Moreover, the experimental results also show that the estimation errors are higher at low temperature conditions. And this result can be explained from the theoretical perspective, the uniformity of the battery surface temperature will deteriorate under low temperature conditions. For comparison, the "8-8-8" GRU-RNN structure with other normalization method in [23], [25] are also be given in Table IV. To gain a better visualization, Fig. 8 plots the comparison results, which clearly show that the proposed method performs more accurately and robustly than other normalization method. For example. the MAE of the proposed method (method 1) and reference method (method 2) testing by US06 under $0°$C is 0.1220 and 0.1237, respectively.

TABLE V
UNCERTAINTY ANALYSIS OF THE GRU-RNN NETWORK WITH FUDS UNDER C

Source	Uncertanty	MEA°C	RMSE°C	MAXE°C
Current	2% (10A)	0.0705	0.0885	0.3219
Voltage	2% (5V)	0.0783	0.0984	0.3468
SOC	Accumulated to 5%	0.0726	0.0928	0.3320
Reference	0	0.0689	0.9877	0.3057

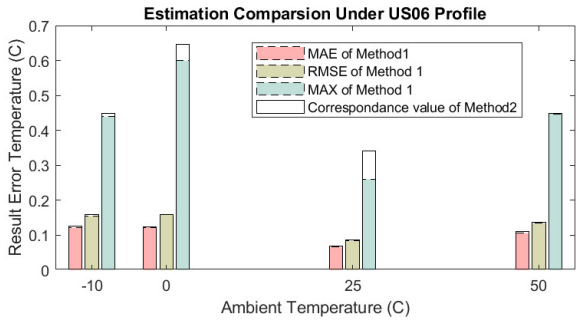

(a)

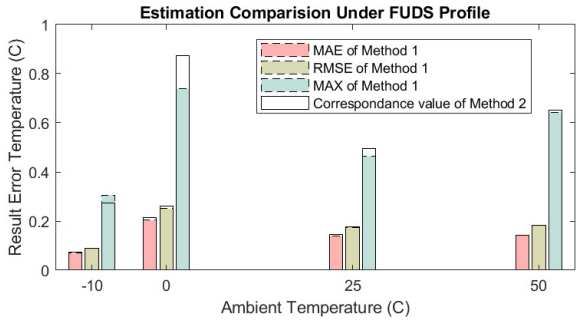

(b)

Fig. 8. The comparison of ST estimation results for Method 1 and Method 2

B. ST Estimation at A Varying Ambient Temperature Condition

However, battery-powered EVs are operated under a continuous temperature changing condition in real situation. Sometimes, EVs can undergo ambient temperature changes of more than 10°C in one day. Therefore, the GRU-RNN network is necessary to be trained and tested under a varying ambient temperature condition, which refers to the dataset2 (from 10°C to 25°C). Moreover, the materials of the sample used in dataset 2 is $LiNiCoAIO_2$, which is different from dataset1 ($LiFePO_4$). Therefore, this experiment not only validates the effectiveness of the proposed GRU-RNN model in a varying temperature environment, but also tests its adaptation ability with different battery materials.

The description of dataset 2 is given in Section IV. The estimation performance of the GRU-RNN with the proposed normalization techniques is shown in Fig.9. The RMSE, MAE and MAX achieved on the dataset2 of the method 1(with the proposed normalization method) are 0.5459°C, 0.4262°C, and 2.5925°C, respectively. For comparison, the GRU-RNN network with the traditional normalization method also be given. The RMSE, MAE and MAX achieved on the dataset2

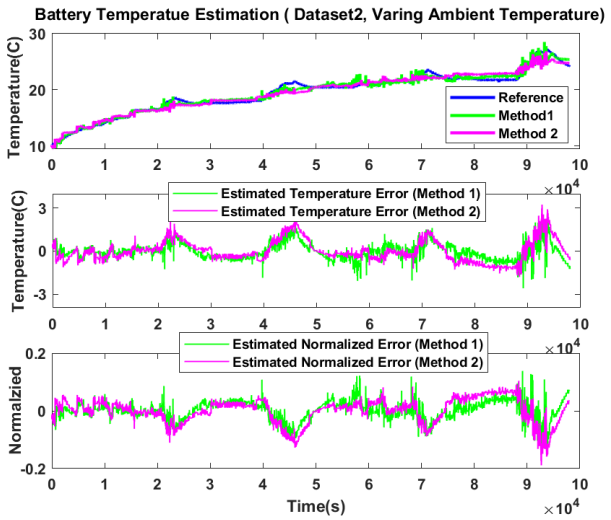

Fig. 9. GRU-RNN network with the proposed normalization method and the reference method are validated under dataset 2 which is operated in a varing ambient temperature condition (from 10°C to 25°C)

of the reference method 2 are 0.7411°C, 0.5676°C, and 3.2463°C, respectively.The results show that the proposed has better performance than the reference method in all compared criteria. However, the GRU-RNN in varing temperature condition shows fluctuations. Especially, the estimation errors are heavily fluctuated at the end of the operation.

C. Uncertainty Analysis

The inputs current, voltage, ambient temperature are measured by physical sensors, The SOC is estimated using these parameters, and SOC estimation is coupled with the temperature. Therefore, it is important to explore the influence of signal measurement errors and SOC estimation errors on ST estimation. Table IV presents an uncertainty analysis of the proposed GRU-RNN network with FUDS under C, the 2% sensor range measurement error is imposed to measured current and voltage, an accumulated error (reaching to 5%) is added to estimated SOC. After adding errors, the estimation accuracy are reduced in all situation, and the 2% uncertainty in voltage measurement has the lowest accuracy in MAE and MAXE.

VI. CONCLUSION

This paper proposes a battery surface temperature estimation method by using a GRU-RNN network with an enhanced normalization method. The network takes current, terminal voltage, ambient temperature, and SOC as input parameters, and the surface temperature as the output. There are three contributions to this work. First, this paper provides the theoretical analysis about the battery surface temperature distribution that it indeed is a typical time (sequence) task, and analyzes the relationship between the surface temperature distribution and RNN. Second, the proposed GRU-RNN network with the enhanced normalization techniques has shown its good performance and generalization ability for different fixed ambient

TABLE VI
COMPARISON OF ST ESTIMATION RESULTS FOR DIFFERENT WORKS

Work	Fixed Ambient Temperatures	Varing Ambient Temperature	Dynamic Loading Profiles	Different Sample Materials	Error
ANN network[1]	25	✗	✗ Constant discharging CCCT dharging	✓ Nickel-metal hydrid (NiMH) Nicker-cadmium (NiCd) Li-ion	<-0.02°C RMSE <0.009°C RMSE <0.006°C RMSE
LSTM-RNN network[7]	-20°C,-10°C,0°C,10°C,25°C	✓ -10°C to 25°C 10°C to 25°C	✓ Combination of UDDS, LA92, US06, HWFET	✗ LiNaCo	<3°C RMSE (fixed) <2°C RMSE (varing)
Impedance Measurement with Kalman Filter[3]	8°C	✗	✓ Artemis HEV drive cycle	✗ LiFePO4	<1.24°C RMSE
ANN+extend Kalman Filter [28]	25°C,40°C	✗	✓ Pulse discharge	✗ Li-ion	<0.20°C MAE
Proposed GRU-RNN network with an enhanced normalization techniques	-10°C, 0°C, 25°C, 50°C	✓ 10 to 25°C	✓ FUDS, US06 Combination of UDDS, LA92, US06, HWFET	✓ LiFePO4 LiNaCo	<0.20 ° C MAE (fixed) <0.42° C MAE (varying)

temperature conditions, varying ambient temperature condition, different chemical materials, and different drive cycles. The proposed GRU-RNN network shows its competitiveness when compared to other methods, as shown in Table VI. Third, an uncertainty analysis is conducted to evaluate the stability and applicability of the proposed GRU-RNN network.

Compared with the traditional model-filter combined method, which requires comprehensive knowledge of the battery characterises and finite-element [6], the proposed method is data-driven and model-free. Moreover, the complication numerical electro-thermal models need a high computational ability, which makes it hard to be implemented online. The machine learning based methods do not require deep understands of chemistry and physics. The model size is acceptable for online computation, and the size can be further reduced by adopting model pruning and quantization techniques [29].

REFERENCES

[1] A. A. Hussein and A. A. Chehade, "Robust artificial neural network-based models for accurate surface temperature estimation of batteries," *IEEE Transactions on Industry Applications*, vol. 56, no. 5, pp. 5269–5278, 2020.

[2] C. G. Moral, D. Fernandez, J. M. Guerrero, D. Reigosa, C. Riva, and F. Briz, "Thermal monitoring of lifepo4 batteries using switching harmonics," *IEEE Transactions on Industry Applications*, 2020.

[3] Y. Xie, R. Yang, W. Li, K. Liu, B. Chen, Y. Qian, and Y. Zhang, "A comprehensive study on influence of battery thermal behavior on degradation and consistency," *IEEE Transactions on Transportation Electrification*, pp. 1–1, 2022.

[4] Q. Zhang, C.-G. Huang, H. Li, G. Feng, and W. Peng, "Electrochemical impedance spectroscopy based state of health estimation for lithium-ion battery considering temperature and state of charge effect," *IEEE Transactions on Transportation Electrification*, pp. 1–1, 2022.

[5] M. Lelie, T. Braun, M. Knips, H. Nordmann, F. Ringbeck, H. Zappen, and D. U. Sauer, "Battery management system hardware concepts: An overview," *Applied Sciences*, vol. 8, p. 534, 2018.

[6] R. R. Richardson and D. A. Howey, "Sensorless battery internal temperature estimation using a kalman filter with impedance measurement," *IEEE Transactions on Sustainable Energy*, vol. 6, no. 4, pp. 1190–1199, 2015.

[7] R. Schwarz, K. Semmler, M. Wenger, V. R. Lorentz, and M. März, "Sensorless battery cell temperature estimation circuit for enhanced safety in battery systems," in *IECON 2015-41st Annual Conference of the IEEE Industrial Electronics Society*. IEEE, 2015, pp. 001 536–001 541.

[8] D. A. Howey, P. D. Mitcheson, V. Yufit, G. J. Offer, and N. P. Brandon, "Online measurement of battery impedance using motor controller excitation," *IEEE Transactions on Vehicular Technology*, vol. 63, no. 6, pp. 2557–2566, 2014.

[9] Q. Yao, D.-D.-C. Lu, and G. Lei, "Accurate online battery impedance measurement method with low output voltage ripples on power converters," *Energies*, vol. 14, no. 4, p. 1064, Feb 2021. [Online]. Available: http://dx.doi.org/10.3390/en14041064

[10] X. Hu, S. E. Li, and Y. Yang, "Advanced machine learning approach for lithium-ion battery state estimation in electric vehicles," *IEEE Transactions on Transportation Electrification*, vol. 2, no. 2, pp. 140–149, 2016.

[11] Y. Guo, Z. Zhao, and L. Huang, "Soc estimation of lithium battery based on improved bp neural network," *Energy Procedia*, vol. 105, pp. 4153–4158, 2017.

[12] E. Chemali, P. J. Kollmeyer, M. Preindl, R. Ahmed, and A. Emadi, "Long short-term memory networks for accurate state-of-charge estimation of li-ion batteries," *IEEE Transactions on Industrial Electronics*, vol. 65, no. 8, pp. 6730–6739, 2017.

[13] F. Yang, S. Zhang, W. Li, and Q. Miao, "State-of-charge estimation of lithium-ion batteries using lstm and ukf," *Energy*, vol. 201, p. 117664, 2020.

[14] V. M. Nagulapati, H. Lee, D. Jung, S. S. Paramanantham, B. Brigljevic, Y. Choi, and H. Lim, "A novel combined multi-battery dataset based approach for enhanced prediction accuracy of data driven prognostic models in capacity estimation of lithium ion batteries," *Energy and AI*, vol. 5, p. 100089, 2021.

[15] M. Naguib, P. Kollmeyer, C. Vidal, and A. Emadi, "Accurate surface temperature estimation of lithium-ion batteries using feedforward and recurrent artificial neural networks," in *2021 IEEE Transportation Electrification Conference Expo (ITEC)*, 2021, pp. 52–57.

[16] F. Yang, W. Li, C. Li, and Q. Miao, "State-of-charge estimation of lithium-ion batteries based on gated recurrent neural network," *Energy*, vol. 175, pp. 66–75, 2019.

[17] K. Cho, B. Van Merriënboer, C. Gulcehre, D. Bahdanau, F. Bougares, H. Schwenk, and Y. Bengio, "Learning phrase representations using rnn encoder-decoder for statistical machine translation," *arXiv preprint arXiv:1406.1078*, 2014.

[18] D. Bernardi, E. Pawlikowski, and J. Newman, "A general energy balance for battery systems," *Journal of the electrochemical society*, vol. 132, no. 1, p. 5, 1985.

[19] Q. Yao, D. D.-C. Lu, and G. Lei, "Rapid open-circuit voltage measurement method for lithium-ion batteries using one-cycle bipolar-current pulse," *IEEE Journal of Emerging and Selected Topics in Industrial Electronics*, vol. 2, no. 2, pp. 132–141, 2020.

[20] S. Haykin and R. Lippmann, "Neural networks, a comprehensive foundation," *International journal of neural systems*, vol. 5, no. 4, pp. 363–364, 1994.

[21] B. Zhang, D. Xiong, J. Su, and H. Duan, "A context-aware recurrent encoder for neural machine translation," *IEEE/ACM Transactions on Audio, Speech, and Language Processing*, vol. 25, no. 12, pp. 2424–2432, 2017.

[22] Y. Bengio, P. Simard, and P. Frasconi, "Learning long-term dependencies with gradient descent is difficult," *IEEE transactions on neural networks*, vol. 5, no. 2, pp. 157–166, 1994.

[23] W. He, N. Williard, C. Chen, and M. Pecht, "State of charge estimation for li-ion batteries using neural network modeling and unscented kalman filter-based error cancellation," *International Journal of Electrical Power & Energy Systems*, vol. 62, pp. 783–791, 2014.

[24] Y. Tian, R. Lai, X. Li, L. Xiang, and J. Tian, "A combined method for state-of-charge estimation for lithium-ion batteries using a long short-term memory network and an adaptive cubature kalman filter," *Applied Energy*, vol. 265, p. 114789, 2020.

[25] C. Bian, H. He, and S. Yang, "Stacked bidirectional long short-term memory networks for state-of-charge estimation of lithium-ion batteries," *Energy*, vol. 191, p. 116538, 2020.

[26] G. Dos Reis, C. Strange, M. Yadav, and S. Li, "Lithium-ion battery data and where to find it," *Energy and AI*, vol. 5, p. 100081, 2021.
[27] M. Youmans, J. C. Spainhour, and P. Qiu, "Classification of antibacterial peptides using long short-term memory recurrent neural networks," *IEEE/ACM Transactions on Computational Biology and Bioinformatics*, vol. 17, no. 4, pp. 1134–1140, 2019.
[28] A. M. Elsergany, A. A. Hussein, A. Wadi, and M. F. Abdel-Hafez, "An adaptive autotuned polynomial-based extended kalman filter for sensorless surface temperature estimation of li-ion battery cells," *IEEE Access*, vol. 10, pp. 14 038–14 048, 2022.
[29] A. Polino, R. Pascanu, and D. Alistarh, "Model compression via distillation and quantization," *arXiv preprint arXiv:1802.05668*, 2018.